Analyst

PAPER

View Article Online
View Journal | View Issue

Cite this: *Analyst*, 2017, **142**, 3740

Target-induced cyclic DNAzyme formation for colorimetric and chemiluminescence imaging assay of protein biomarkers†

Kaili Yang, Min Huo, Yuehua Guo, Yizhuo Yang, Jie Wu, * Lin Ding* and Huangxian Ju

Received 9th March 2017,
Accepted 15th August 2017

DOI: 10.1039/c7an00413c

rsc.li/analyst

A target-induced cyclic strategy for DNAzyme formation was proposed to achieve simple, sensitive and universal detection of protein biomarkers with convenient colorimetric or chemiluminescence imaging readout. In the assay, the target protein was recognized by a pair of DNA-labeled antibodies (Ab1-DNA1 and Ab2-DNA2) to form a proximate complex, which could hybridize with the conjugate DNA3/DNA4 to release the guanine-rich DNA4 and thus formed G-quadruplex/hemin horseradish peroxidase-mimicking DNAzyme. The process could be further recycled with Exonuclease III by cleaving DNA3 to free the proximate complex, resulting in the cyclic formation of DNAzyme. The G-quadruplex/hemin DNAzyme could catalyze the H_2O_2-mediated oxidation of 3,3,5,5-tetramethylbenzidine to produce the color change from colorless to blue or enhance the chemiluminescence of a luminol–H_2O_2 system. Thus the signal could be read out with the naked eye, and by colorimetry and chemiluminescence imaging. Using a carcinoembryonic antigen as a model target, the proposed assay showed a detection range of 4 orders of magnitude along with detection limits of 170 and 16 pg mL^{-1} for colorimetric and chemiluminescence imaging assays respectively. This assay had the advantages of easy operation, sensitive detection, target flexibility and diversified signal readout, providing a great opportunity for commercial application.

Introduction

As the levels of tumor biomarkers in human serum are closely related to the stages of tumors,[1–3] it is extremely important to develop simple, low cost, rapid, sensitive, and selective assays to monitor disease-related proteins for early diagnosis and treatment of cancers. In recent years, various immunoassay methods such as enzyme-linked immunosorbent assays (ELISA),[4] electrochemical immunoassays,[5,6] fluoroimmunoassays,[7,8] chemiluminescence (CL) immunoassays[9,10] and colorimetric immunoassays[11,12] have been developed to detect protein biomarkers. Although these assays can provide a high detection sensitivity, most of them follow a multi-step heterogeneous detection format and are carried out on precision solid substrates, leading to high cost, time consumption and labor waste. Thus wash-free and one-step homogeneous methods have been considered for simple and efficient detection of protein biomarkers to achieve point-of-care testing.

Colorimetric immunoassays have received great attention owing to the advantages of simplicity, low cost and practicality.[13,14] Particularly, naked-eye readout can achieve semiquantitative assessment in real time, which is crucial for field tests and point-of-care diagnosis. In colorimetric immunoassay, the enzyme labeled on the second antibody catalyzes the chromogenic agents to produce a color change from colorless to blue or green color, which leads to the detection of the target at the ng mL^{-1} level with the naked eye.[15,16] In order to enhance the detection sensitivity, plasmonic colorimetry has been developed, in which the enzyme catalyzes the growth or etching of plasmonic nanostructures such as gold or silver nanoparticles, resulting in the modification of their size, shape, distribution, or metal composition and hence the color change.[17,18] Although these assays can drop the detection limit down to the attomolar level, some physical and chemical factors such as pH value, ionic strength, temperature and other impurities greatly affect the aggregation of nanoparticles and the bioactivity of most natural enzymes.[19] In addition, the labelling process of enzymes is laborious and also easy to affect the catalytic activity of enzymes since the modification on enzymes has a high probability of approaching the enzymatic active site or hindering substrate proximity to the active center.[20] These reasons inevitably influence the accuracy and reproducibility

State Key Laboratory of Analytical Chemistry for Life Science, School of Chemistry and Chemical Engineering, Nanjing University, Nanjing 210023, P.R. China. E-mail: wujie@nju.edu.cn, dinglin@nju.edu.cn; Fax: +86 25 89681923

†Electronic supplementary information (ESI) available. See DOI: 10.1039/c7an00413c

of colorimetric immunoassays, and thus limit their application in real sample assay. So, adopting a novel design to construct nanoparticle-free and label-free visual detection platforms is very desirable.

The G-quadruplex/hemin DNAzyme, a horseradish peroxidase-mimicking DNAzyme, can catalyze various H_2O_2-mediated biochemical reactions and has been widely used in bioanalysis and clinical diagnoses,[21,22] in virtue of its good stability, low cost, easy preparation and modification, and adjustable enzymatic activities with particular cofactors. However, the catalytic activity of the G-quadruplex/hemin DNAzyme is not as satisfactory as horseradish peroxidase. Thus, a series of signal amplification strategies have been designed to prepare a multi-DNAzyme nanostructure or *in situ* synthesize multiple DNAzymes by various DNA assembly[23,24] and enzymatic recycling techniques.[25] Recently, Exonuclease III (Exo III) has been widely used for catalytic DNA assembly because it does not require a specific recognition site. Exo III can specifically digest double-stranded DNA (dsDNA) from the 3′-OH blunt or recessed end, but exhibits less activity on single stranded DNA or 3′-overhang ends of double-stranded DNA.[26] For example, a cascade signal amplification strategy has been reported to produce multiple G-quadruplex/hemin DNAzymes by two Exo III-assisted cycling processes and construct the ultrasensitive CL assay of DNA.[27] Here, by combining DNA proximate hybridization and displacement assembly with Exo III-assisted enzymatic recycling, a target-induced cyclic DNAzyme formation strategy was proposed for simple and sensitive detection of protein biomarkers.

Proximate hybridization is a sandwich affinity binding-induced DNA assembly strategy, in which a pair of DNA-conjugated affinity probes simultaneously recognize the target and subsequently induce the hybridization of DNA labels to trigger cascade DNA assembly and the detection signals.[28] As proximate hybridization can perform homogenously, it has been introduced to construct various electrochemical,[5,6] fluorescent,[29,30] and CL immunoassays[31] for one-step protein detection. In this work, proximate hybridization was designed to regulate the *in situ* formation of the G-quadruplex/hemin DNAzyme, and homogenous colorimetric and chemiluminescence imaging assay of the carcinoembryonic antigen (CEA) was constructed. The presented assay showed the appealing features of (1) simple operation, the assay was homogeneous and could be carried out without separation and washing steps; (2) target flexibility, the assay could be applied to detect a variety of proteins by using the corresponding affinity recognition pairs; (3) sensitive detection, by introducing Exo III-assisted enzymatic recycling, the signal of the assay was greatly amplified and a detection limit at the sub-ng mL^{-1} level could be obtained with the naked eye; (4) convenient signal readout, the signal could be detected with the naked eye, colorimetry and chemiluminescence imaging according to the color development reaction or CL reaction catalyzed by the G-quadruplex/hemin DNAzyme. Thus, the proposed assay met greatly the requirements of point-of-care testing, showing a wide application prospect.

Experimental

Materials and reagents

The oligonucleotides used in this work are shown in Table S1,† which were synthesized and purified employing HPLC by Sangon Biological Engineering Technology & Co. Ltd (Shanghai, China). The complementary bases of DNA2 to DNA1 are shown in green with bold, and the hybridization bases between DNA3 and DNA4 are shown in blue with bold. CEA, anti-CEA antibody (mouse monoclonal antibodies, Ab1 and Ab2, clone no. Z-2011 and Z-2012) and α-fetoprotein (AFP) were obtained from Beijing Keybiotech Co. Ltd (China). Hemin, brilliant blue R, maleimidobenzoic acid *N*-hydroxysuccinimide ester (MBS), and tris(2-carboxyethyl)phosphine hydrochloride (TCEP) were purchased from Sigma-Aldrich (St Louis, MO, USA). The stock solutions of hemin (100 mM) and MBS (6.4 mM) were prepared in dimethyl sulphoxide (DMSO), respectively. The color development solution containing 3,3,5,5-tetramethylbenzidine (TMB) and H_2O_2 was obtained from Beyotime (Jiangsu, China). CL substrate solution containing luminol–*p*-iodophenol and H_2O_2 was purchased from Autobio Diagnostics Co. Ltd (China). Exo III was purchased from Takara Biotechnology Co. Ltd (Dalian, China). All other reagents were of analytical grade and used without further purification. Ultrapure water used in all experiments was obtained from a Millipore water purification system (≥18 MΩ, Milli-Q, Millipore). TE buffer (20 mM Tris-HCl, 150 mM KCl and 15 mM $MgCl_2$, pH 8.0) was used as the stock solution and reaction buffer of oligonucleotides. The clinical serum samples were obtained from Jiangsu Cancer Hospital. Here, the blood samples obtained from patients were firstly processed for serum at 3000 rpm for 10 min at 4 °C to completely remove cellular components after 20 min of collection, and then stored at −20 °C before use.

Apparatus

An electrophoresis analyser (Bio-Rad, USA) and Bio-rad ChemDoc XRS (Bio-Rad, USA) were used to carry out polyacrylamide gel electrophoresis (PAGE) analysis and imaging, respectively. Ultraviolet-visible (UV-vis) absorption spectra were recorded with a Varioskan Flash multimode reader (Thermo Scientific, USA). CL images were collected by using a high resolution cooled low-light CCD (BioImaging Systems Chemi HR 410 camera, UVP, USA).

Preparation of DNA-labeled antibody

MBS was used as a bio-functional linker to conjugate DNA and the antibody, according to the previous work.[32] Firstly, 20 μL of 2 mg mL^{-1} anti-CEA was treated with a 40-fold molar excess of MBS in 10 mM PBS at pH 7.2 for 2 h and the superfluous MBS was removed by ultrafiltration (100 kDa Millipore, 10 000 rpm). Meanwhile, 24 μL of 100 μM thiolated oligonucleotide was reduced with a 150-fold molar excess of TCEP in 10 mM PBS at pH 5.5 for 2 h at room temperature and purified by ultrafiltration (10 kDa Millipore, 10 000 rpm) with 10 mM PBS (pH 7.2). Then, the reduced thiol-DNA was mixed with the pur-

ified anti-CEA-MBS for 2-h incubation at room temperature. The Ab-DNA conjugate was obtained after removing the unreacted thiol-DNA by ultrafiltration (100 kDa Millipore, 10 000 rpm) and stored in 66 μL PBS (10 mM, pH 7.2).

PAGE and Coomassie Brilliant Blue analysis

The native polyacrylamide gel (12%) was prepared with Tris-Borate-EDTA (TBE) buffer. The loading sample was a mixture of 3.5 μL of DNA or a DNA-based substrate, 0.75 μL of UltraPower™ dye, and 0.75 μL of 6× loading buffer, and it was kept for 3 min to ensure the combination of the dye with DNA before injection. After 75 min of electrophoretic analysis at 100 V, the gel was illuminated with UV light and photographed with a Molecular Imager Gel Doc XR. After electrophoresis, the gel was stained for 1 h with 0.025% (w/v) Coomassie Brilliant Blue R-250 dye, and then destained for 5 h with an aqueous solution containing methanol and acetic acid. The gel was photographed with a commercial camera.

Colorimetric detection of CEA

The colorimetric detection was performed on a 96 well plate (Scheme 1), and each well was used as a detection cell for CEA. In each well, 2 μL of various concentrations of CEA or serum samples was mixed with 18 μL of affinity recognition solution containing DNA3/DNA4 double strand (ds-DNA3/DNA4), hemin, Exo III, and the pair of Ab-DNA conjugates with the final concentrations of 2 μM, 5 μM, 0.4 U μL^{-1}, and 0.25 μM, respectively. After 30-min incubation in the dark at 37 °C, 180 μL of color development solution was added to the mixture and incubated for 20 min in the dark for colorimetric reaction. The color change could be directly observed with the naked eye or detected by using a microplate reader at 652 nm.

CL imaging assay of CEA

Similar to the colorimetric detection, 0.5 μL of target protein or serum samples was firstly reacted with 4.5 μL of affinity recognition solution for 30 min. Then, 45 μL of CL substrate solution was added to the mixture to generate the CL signal, which was immediately recorded by a CCD with a 15 s dynamic integration and automatically identified by VisionWorksLS image acquisition and analysis software (UVP). The CL intensity of each well was calculated as the mean pixel intensity within a circle of a given radius around each spot center.

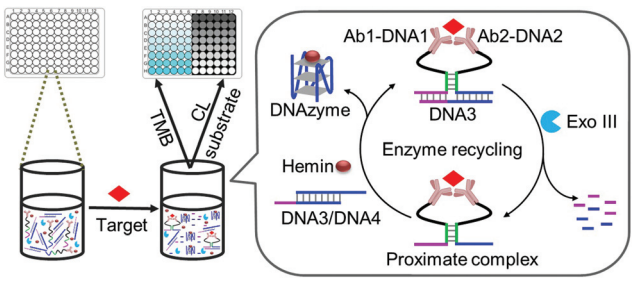

Scheme 1 Schematic illustration of the colorimetric and CL imaging assay of proteins based on target-induced cyclic DNAzyme formation.

Results and discussion

Design of target-induced cyclic DNAzyme formation

In the proposed assay, a pair of DNA-labeled antibodies (Ab1-DNA1 and Ab2-DNA2), ds-DNA (DNA3/DNA4) and Exo III were engineered to perform the target recognition and signal amplification (Scheme 1). Here, DNA1 only contained 6 complementary bases to DNA2, thus DNA1 could not hybridize with DNA2 without the help of the proximity effect. In ds-DNA, part of DNA3 hybridized with DNA4, and the 3′ end of DNA3 was overhung. The simultaneous affinity recognition of the target protein with the pair of DNA-labeled antibodies brought the DNA1 and DNA2 in close proximity for hybridization, which formed the proximate complex (Ab1-DNA1/Target/Ab2-DNA2), and could subsequently hybridize with DNA3 to release guanine-rich DNA4, leading to the formation of the G-quadruplex/hemin DNAzyme. As the 3′ end of DNA3 was changed from overhang to recess during the displacement hybridization, it could be cleaved by Exo III from the proximate complex. The free proximate complex could further hybridize with another DNA3, and release another DNA4 to form more DNAzymes, which amplified the colorimetric and CL signal.

Feasibility of the proposed strategy

In order to testify the feasibility of this strategy, a DNA strand with 80 bases (DNA5) was used to mimic the Ab1-target-Ab2 complex[33] and perform the proximate hybridization followed by displacement hybridization (Fig. 1A). These hybridization processes were monitored with PAGE analysis (Fig. 1B). As DNA5 contained 18 bases complementary to both DNA1

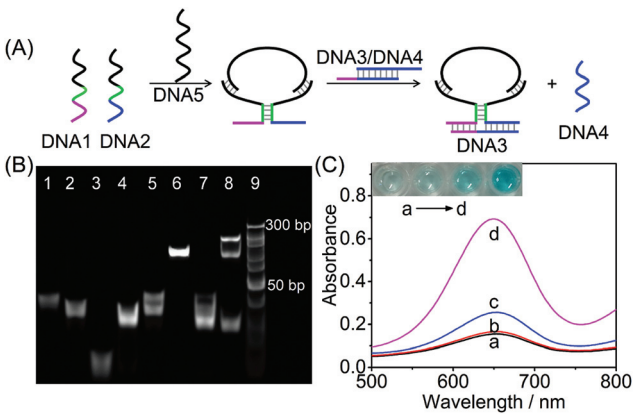

Fig. 1 (A) Schematic illustration of target-induced hybridization and (B) corresponding PAGE analysis. Lane 1: DNA1, lane 2: DNA2, lane 3: DNA4, lane 4: DNA3/DNA4, lane 5: mixture of DNA1 and DNA2, lane 6: mixture of DNA1, DNA2 and DNA5, lane 7: mixture of DNA1, DNA2 and DNA3/DNA4, lane 8: mixture of DNA1, DNA2, DNA5 and DNA3/DNA4, lane 9: DNA marker. (C) UV absorption spectra of the (a) mixture of hemin, Ab1-DNA1, Ab2-DNA2, and DNA3/DNA4, (b) (a) + 0.4 U μL^{-1} of Exo III, (c) (a) + 50 ng mL^{-1} CEA, (d) (c) + 0.4 U μL^{-1} of Exo III.

and DNA2, the mixture of DNA5 with DNA1 and DNA2 could produce a hybridization complex of DNA1/DNA5/DNA2 (lane 6), which moved slower than DNA1 (and DNA2) (lanes 1, 2 and 5). In the absence of DNA5, the mixture of DNA1, DNA2 and DNA3/DNA4 (lane 7) showed bands located at the same position as DNA1 (and DNA2) (lane 5), and DNA3/DNA4 (lane 4), respectively, indicating that no hybridization occurred among DNA1, DNA2 and DNA3/DNA4. After adding DNA5 to the mixture of DNA1, DNA2 and DNA3/DNA4 (lane 8), the band referring to the DNA1/DNA5/DNA2 complex (lane 6) was observed along with a new band at slower migration. The new band was attributed to the formation of the DNA1/DNA5/DNA2/DNA3 complex, verifying the occurrence of the proximate hybridization between DNA1 and DNA2 and the subsequent displacement hybridization of the DNA1/DNA5/DNA2 complex with DNA3. Here, since this displacement hybridization did not occur completely, the amount of released DNA4 cannot be seen in lane 8.

The feasibility of the target-induced cyclic DNAzyme formation strategy was further investigated by colorimetric detection (Fig. 1C). In the absence of the target, DNA1 and DNA2 could not be brought close enough to hybridize each other to form the proximate complex and induce DNAzyme formation. Thus, the chromogenic reaction did not occur and the solution without or with Exo III was colorless (a and b, insert of Fig. 1C). Correspondingly, relatively low absorption intensities were observed at 652 nm (curves a and b), which could be denoted as the background. The slight color change of the background solution as well as the background intensity was attributed to the existence of hemin. After adding 50 ng mL^{-1} CEA to the affinity recognition solution, a blue color of the solution with 35% increase of the absorption intensity at 652 nm was observed (c, Fig. 1C) due to the target-induced formation of the G-quadruplex/hemin DNAzyme. By introducing Exo III into the system, the color of the solution became dark blue, and 325% increase of the absorption intensity was obtained (d, Fig. 1C). The amplified signal was attributed to the plentiful DNAzymes produced by Exo III-assisted enzymatic recycling. These results indicated the feasibility of the target-induced cycle for DNAzyme formation and its application for the sensitive detection of protein markers.

Characterization of Ab-DNA conjugate

PAGE analysis was employed to verify the formation of the Ab-DNA conjugate (Fig. 2A and B). The mixture of Ab1 and DNA1 showed a bright band (Fig. 2A, lane 3) at the same position as DNA1 (Fig. 2A, lane 1), suggesting that DNA1 could not conjugate with Ab1 without MBS coupling. Contrarily, a band of DNA was observed to be stuck on the well of the prepared Ab1-DNA1 conjugate (Fig. 2A, lane 4), which was attributed to its large molecular weight after coupling with Ab.[34] Here, the location of the DNA band was in agreement with that of the Ab band in the protein-staining image (Fig. 2B, lane 4), confirming the successful preparation of the Ab-DNA conjugate. From the UV-vis absorbance ratio of Ab-DNA at 260 nm to 280 nm

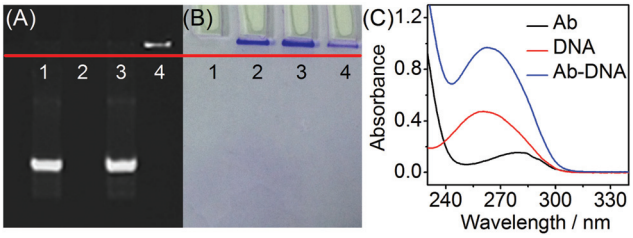

Fig. 2 (A) Native PAGE and (B) protein-staining images of DNA1 (lane 1), Ab1 (lane 2), mixture of DNA1 and Ab1 (lane 3), and Ab1-DNA1 conjugate (lane 4). (C) UV absorption spectra of Ab, DNA and Ab-DNA.

(Fig. 2C), the number of DNA bound on each Ab could be calculated to be 5.[35]

Optimization of detection conditions

The successful detection of the target protein depends on the efficient operation of target-induced proximity hybridization, displacement hybridization triggered DNAzyme formation, and Exo III based enzymatic recycling. Thus, the conditions including the sequence of DNA4, the stability of ds-DNA3/DNA4, the number of complementary bases between DNA1 and DNA2, the amount of Exo III, and the reaction time of the assay were optimized. The G-quadruplex/hemin DNAzyme could be produced spontaneously at the coexistence of a guanine-rich sequence and hemin, however, the catalytic activity of the DNAzyme depended on the sequence of guanine-rich DNA.[36] As shown in Fig. 3, the absorbance obtained with a general guanine-rich sequence (DNA4 (1))[21] was 4.6 and 3.5 times lower than that from the DNAzyme formed with the guanine-rich sequences with 3 cytosine modifications at both ends of DNA4 (2) and (3), respectively, indicating that the DNAzyme formed with the C modified guanine-rich sequence possessed high catalytic activity.[36] In the proposed assay, guanine-rich DNA4 was presented on ds-DNA3/DNA4 and released by the displacement hybridization. Thus, the stability of ds-DNA3/DNA4 should be optimized to ensure the release of DNA4 by the proximate complex instead of

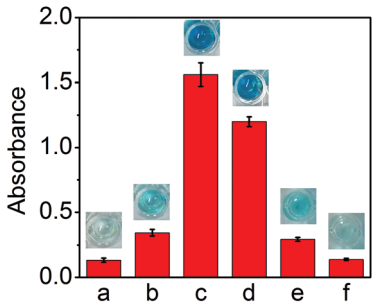

Fig. 3 Sequence optimization of DNA4 and ds-DNA3/DNA4. Hemin (a), the mixture of hemin with DNA4 (1) (b), DNA4 (2) (c), DNA4 (3) (d), ds-DNA3(2)/DNA4(2) (e) and ds-DNA3(3)/DNA4(3) (f), respectively. The concentration of hemin, DNA4 and ds-DNA3/DNA4 was 500, 100 and 200 nM, respectively.

hemin. As a control, ds-DNA3(2)/DNA4(2) and ds-DNA3(3)/DNA4(3), containing 16 and 23 complementary bases, were studied. A bright blue color was observed from the color development solution incubated in the mixture of ds-DNA3(2)/DNA4(2) and hemin, indicating that DNA4 could be directly released from ds-DNA3(2)/DNA4(2) to form DNAzyme. However, the color and the absorbance of the ds-DNA3(3)/DNA4(3)-based solution were similar to the background hemin solution. This result illustrated that the ds-DNA3(3)/DNA4(3) was stable and DNA4 could not be released by hemin without the help of the proximate complex. Thus, ds-DNA3(3)/DNA4(3) was used in the whole assay.

The complementary length of DNA1 and DNA2 determined the success of the proximity hybridization process. Too many complementary bases caused self-hybridization of DNA1 and DNA2, however too little complementary bases made the hybridization of DNA1 and DNA2 difficult even in the presence of the target. As shown in Fig. 4A, by increasing the number of complementary bases in DNA1 and DNA2, the signal was increased sharply to attain the maximum value at 6 base pairs and then trended to be gentle, however the noise consistently increased since the complementary base number increased from 4 to 10. Considering the signal-to-noise ratio, 6 complementary bases were selected for the assay.

For the enzymatic recycling amplification, the amount of Exo III was also optimized. Obviously, with the increasing concentration of Exo III, the signal increased and reached a plateau at 0.4 U μL^{-1}, while the noise was almost constant (Fig. 4B). Thus, 0.4 U μL^{-1} Exo III was used for the assay. In addition, the effect of the incubation time was also examined (Fig. 4C). The signal reached the maximum value at the incubation time of up to 30 min, demonstrating that 30 min incubation was enough for the experiment. Furthermore, the reaction time of the color development reaction was optimized (Fig. 4D). According to the signal-to-noise ratio, an optimal time of 20 min was chosen for the color development.

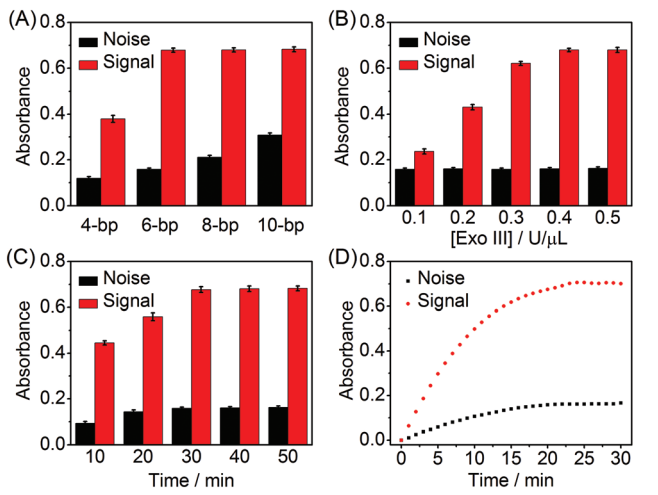

Fig. 4 Optimization of (A) complementary base number between DNA1 and DNA2, (B) amount of Exo III, (C) incubation time and (D) color development time of the assay at 50 ng mL^{-1} CEA.

Analytical performance

Under the optimal conditions, the color changed gradually to deep blue with the increasing concentration of CEA, and the color difference from 200 pg mL^{-1} to 100 ng mL^{-1} CEA could be distinguished easily with the naked eye (Fig. 5A). Furthermore, the CEA concentration could be quantitatively detected by recording the absorbance at 652 nm using a microplate reader. The absorbance proportionally increased with the increasing CEA concentration (Fig. 5B). The absorbance was in log-linear correlation with the CEA concentration over a range from 200 pg mL^{-1} to 1000 ng mL^{-1}, and the linear regression equation was $A = 0.1898 \log[C] + 0.3358$ with a correlation coefficient of 0.9962 (Fig. 5C). The limit of detection (LOD) for CEA was calculated to be 170 pg mL^{-1} (~0.85 pM), corresponding to the signal of the blank plus 3 times standard deviation. The LOD was 100 times lower than that of the catalytic DNA hairpin assembly-based immunoassay,[37] 10 times lower than the nicking endonuclease amplified fluorescence immunoassay,[38] and also much lower than other colorimetric methods by using hybridization assembly-[39] and hybridization chain reaction-assisted[40] DNAzyme formation amplification.

Due to the catalytic ability of the G-quadruplex/hemin DNAzyme towards the luminol–H_2O_2 system, the proposed assay could facilitate detection with CL imaging readout. After the reaction with the target, the CL substrate was added for the immediate generation of the CL signal, which could be

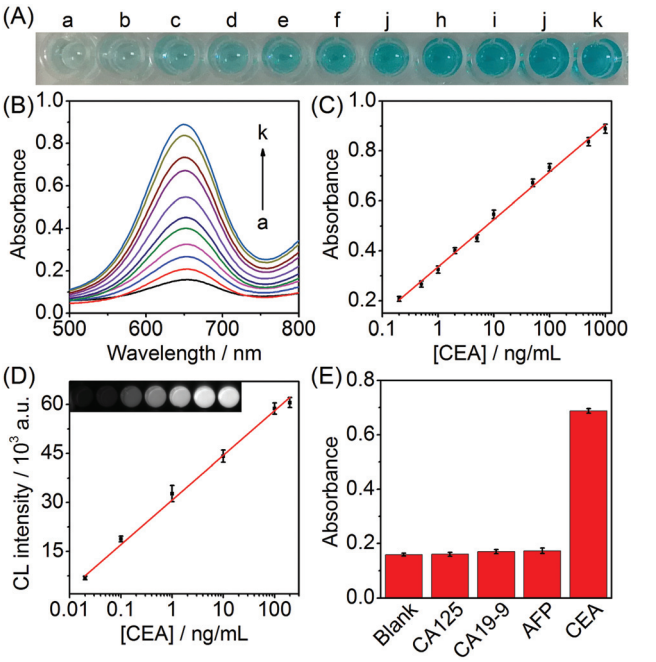

Fig. 5 Analysis of CEA with the (A) naked eye and (B) microplate reader at different concentrations: (a–k) 0, 0.2, 0.5, 1, 2, 5, 10, 50, 100, 500, 1000 ng mL^{-1}. (C) Plot of absorbance at 652 nm *vs.* logarithm of CEA concentration. (D) The CL imaging assay of CEA at 0, 0.02, 0.1, 1, 10, 100 and 200 ng mL^{-1} and the corresponding calibration curve. (E) Specificity of the colorimetric assay using 100 U mL^{-1} CA 125, 100 U mL^{-1} CA 19-9, 100 ng mL^{-1} AFP, and 50 ng mL^{-1} CEA.

recorded by using a CCD (Fig. 5D). The intensity was linearly proportional to the logarithm value of the CEA concentration over the range of 20 pg mL^{-1} to 200 ng mL^{-1} with the linear regression equation of $I = 13.66 \log[C] + 30.73$. A limit of detection of 16 pg mL^{-1} (80 fM) corresponding to the signal of the blank plus 3 times standard deviation was obtained, which was 10 times lower than the colorimetric detection described above. These results demonstrated that the strategy with target-induced cyclic DNAzyme formation could be used for efficient and sensitive detection of proteins with different signal readouts.

By comparing the absorbance of the solutions containing CA 125, CA 19-9, AFP, and CEA at 652 nm (Fig. 5E), the specificity of the proposed assay was evaluated. In the presence of AFP with a concentration much higher than CEA, the signal for CEA was slightly changed, demonstrating the good specificity of the proposed assay.

Real sample analysis

For practical application, the strategy should have the ability to accurately detect target proteins in the real bio-environment. Here, the analysis of CEA in clinical serum samples was performed by the proposed assay strategy with both colorimetric and CL detections and the results are shown in Table S2.† Compared with the reference values from the commercial electrochemiluminescence detection, the relative errors were less than 8.66%, revealing the good reliability of the proposed assay. Therefore, this economical strategy with one-step operation is an ideal candidate for commercial ELISA testing.

Conclusions

This work proposes a strategy for target-induced *in situ* cycling DNAzyme formation, which leads to a simple, sensitive and universal assay for colorimetric and CL detection of protein biomarkers. Different from the traditional ELISA using enzyme-labeled Ab, the proposed assay contains target-induced cascade DNA hybridization to *in situ* produce DNAzyme, which avoids the enzyme labelling process and makes the assay simple and cost-efficient. In addition, benefiting from the proximate recognition, the assay can be performed homogenously without separation and washing, and thus can be easily operated for point of care testing. Moreover, Exo III-assisted signal amplification provides the assay with a high sensitivity and it achieves a detection limit down to the fM level. The proposed assay could be conveniently extended to detect a variety of protein biomarkers by using the corresponding Abs. Overall, the simple and sensitive assay strategy along with diversified signal readout largely meets the point-of-care analysis, showing great potential application in cancer diagnosis.

Conflicts of interest

There are no conflicts of interest to declare.

Acknowledgements

We gratefully acknowledge the National Natural Science Foundation of China (21575063 and 21361162002), the Program for New Century Excellent Talents in the University of Ministry of Education of China (NCET-13-0283) and the Independent Research Foundation from the State Key Laboratory of Analytical Chemistry for Life Science (5431ZZXM1610).

References

1 D. Sidransky, *Nat. Rev. Cancer*, 2002, **2**, 210–219.
2 J. Wu, F. Yan, X. Q. Zhang, Y. T. Yan, J. H. Tang and H. X. Ju, *Clin. Chem.*, 2008, **54**, 1481–1488.
3 J. D. Wulfkuhle, L. A. Liotta and E. F. Petricoin, *Nat. Rev. Cancer*, 2003, **3**, 267–275.
4 B. Y. Cao, G. Z. He, H. Yang, H. F. Chang, S. Q. Li and A. P. Deng, *Talanta*, 2013, **115**, 624–630.
5 J. M. Hu, T. Y. Wang, J. Kim, C. Shannon and C. J. Easley, *J. Am. Chem. Soc.*, 2012, **134**, 7066–7072.
6 J. M. Hu, Y. J. Hu, J. C. Brooks, L. A. Godwin, S. Somasundaram, F. Torabinejad, J. Kim, C. Shannon and C. J. Easley, *J. Am. Chem. Soc.*, 2014, **136**, 8467–8474.
7 F. Li, H. Q. Zhang, C. Lai, X. F. Li and X. C. Le, *Angew. Chem., Int. Ed.*, 2012, **51**, 9317–9320.
8 R. Hu, T. Liu, X. B. Zhang, Y. H. Yang, T. Chen, C. C. Wu, Y. Liu, G. Z. Zhu, S. Y. Huan, T. Fu and W. H. Tan, *Anal. Chem.*, 2015, **87**, 7746–7753.
9 C. Zong, J. Wu, J. Xu, H. X. Ju and F. Yan, *Biosens. Bioelectron.*, 2013, **43**, 372–378.
10 Z. J. Yang, Y. Cao, J. Li, J. T. Wang, D. Du, X. Y. Hua and Y. H. Lin, *Chem. Commun.*, 2015, **51**, 14443–14446.
11 J. J. Liang, C. Z. Yao, X. Q. Li, Z. Wu, C. H. Huang, Q. Q. Fu, C. F. Lan, D. L. Cao and Y. Tang, *Biosens. Bioelectron.*, 2015, **69**, 128–134.
12 C. Li, Y. C. Yang, D. Wu, T. Q. Li, Y. M. Yin and G. X. Li, *Chem. Sci.*, 2016, **7**, 3011–3016.
13 L. Zhan, C. M. Li, W. B. Wu and C. Z. Huang, *Chem. Commun.*, 2014, **50**, 11526–11528.
14 Z. Q. Gao, K. C. Deng, X. D. Wang, M. Miró and D. P. Tang, *ACS Appl. Mater. Interfaces*, 2014, **6**, 18243–18250.
15 Z. Q. Gao, M. D. Xu, L. Hou, G. N. Chen and D. P. Tang, *Anal. Chim. Acta*, 2013, **776**, 79–86.
16 Z. Q. Gao, L. Hou, M. D. Xu and D. P. Tang, *Sci. Rep.*, 2014, **4**, 3966.
17 M. P. N. Bui, S. Ahmed and A. Abbas, *Nano Lett.*, 2015, **15**, 6239–6246.
18 R. de la Rica and M. M. Stevens, *Nat. Nanotechnol.*, 2012, **7**, 821–824.
19 D. B. Liu, Z. T. Wang, A. Jin, X. L. Huang, X. L. Sun, F. Wang, Q. Yan, S. X. Ge, N. S. Xia, G. Niu, G. Liu, A. R. Hight Walker and X. Y. Chen, *Angew. Chem., Int. Ed.*, 2013, **52**, 14065–14069.

20 Z. Y. Zhang, Z. P. Chen, S. S. Wang, F. B. Cheng and L. X. Chen, *ACS Appl. Mater. Interfaces*, 2015, **7**, 27639–27645.
21 A. Niazov-Elkan, E. Golub, E. Sharon, D. Balogh and I. Willner, *Small*, 2014, **10**, 2883–2891.
22 T. Hou, X. Z. Wang, X. J. Liu, S. F. Liu, Z. F. Du and F. Li, *Analyst*, 2013, **138**, 4728–4731.
23 S. Shimron, F. Wang, R. Orbach and I. Willner, *Anal. Chem.*, 2012, **84**, 1042–1048.
24 K. Shi, B. T. Dou, J. M. Yang, R. Yuan and Y. Xiang, *Anal. Chim. Acta*, 2016, **916**, 1–7.
25 T. T. Qiu, Y. Wang, J. H. Yu, S. Liu, H. Z. Wang, Y. N. Guo and J. D. Huang, *RSC Adv.*, 2016, **6**, 62031–62037.
26 I. R. Lehman and C. C. Richardson, *J. Biol. Chem.*, 1964, **239**, 233–241.
27 Y. Gao and B. X. Li, *Anal. Chem.*, 2014, **86**, 8881–8887.
28 M. M. Liu, J. Wu, K. L. Yang, C. Zong, J. P. Lei and H. X. Ju, *Talanta*, 2016, **154**, 455–460.
29 H. Q. Zhang, M. Lai, A. Zuehlke, H. Y. Peng, X. F. Li and X. C. Le, *Angew. Chem., Int. Ed.*, 2015, **54**, 14326–14330.
30 F. Li, H. Q. Zhang, Z. X. Wang, X. K. Li, X. F. Li and X. C. Le, *J. Am. Chem. Soc.*, 2013, **135**, 2443–2446.
31 C. Zong, J. Wu, M. M. Liu, L. L. Yang, L. Liu, F. Yan and H. X. Ju, *Anal. Chem.*, 2014, **86**, 5573–5578.
32 K. Tram, P. Kanda, B. J. Salena, S. Y. Huan and Y. F. Li, *Angew. Chem., Int. Ed.*, 2014, **53**, 12799–12802.
33 K. W. Ren, J. Wu, F. Yan and H. X. Ju, *Sci. Rep.*, 2014, **4**, 4360.
34 Y. Xiang and Y. Lu, *Nat. Chem.*, 2011, **3**, 697–703.
35 Z. J. Zhou, Y. Xiang, A. J. Tong and Y. Lu, *Anal. Chem.*, 2014, **86**, 3869–3875.
36 T. J. Chang, H. M. Gong, P. Ding, X. J. Liu, W. G. Li, T. Bing, Z. H. Cao and D. H. Shangguan, *Chem. – Eur. J.*, 2016, **22**, 1–8.
37 Y. N. Tang, Y. W. Lin, X. L. Yang, Z. X. Wang, X. C. Le and F. Li, *Anal. Chem.*, 2015, **87**, 8063–8066.
38 B. Deng, J. B. Chen and H. Q. Zhang, *Anal. Chem.*, 2014, **86**, 7009–7016.
39 H. Wu, K. Zhang, Y. L. Liu, H. Y. Wang, J. Wu, F. F. Zhu and P. Zou, *Biosens. Bioelectron.*, 2015, **64**, 572–578.
40 Y. Zhang, W. Ren, H. Q. Luo and N. B. Li, *Biosens. Bioelectron.*, 2016, **80**, 463–470.